CA3 NMDA Receptors are Required for Experience-Dependent Shifts in Hippocampal Activity

Kelly Kent,[1] Kenneth Hess,[1] Susumo Tonegawa,[2] and Scott A. Small[1]*

ABSTRACT: The anatomical distribution of sensory-evoked activity recorded from the hippocampal long-axis can shift depending on prior experience. In accordance with Marr's computational model of hippocampal function, CA3 NMDA receptors have been hypothesized to mediate this experience-dependent shift in hippocampal activity. Here we tested this hypothesis by investigating genetically-modified mice in which CA3 NMDA receptors are selectively knocked-out (CA3-NR1 KO). First, we were required to develop an fMRI protocol that can record sensory-evoked activity from the mouse hippocampal long-axis. This goal was achieved in part by using a dedicated mouse scanner to image odor-evoked activity, and by using non-EPI (echo planer imaging) pulse sequences. As in humans, odors were found to evoke a ventral-predominant activation pattern in the mouse hippocampus. More importantly, odor-evoked activity shifted in an experience-dependent manner. Finally, we found that the experience-dependent shift in hippocampal long-axis activity is blocked in CA3-NR1 knock-out mice. These findings establish a cellular mechanism for the plasticity imaged in the hippocampal long-axis, suggesting how experience-dependent modifications of hippocampal activity can contribute to its mnemonic function.

KEY WORDS: CA3 neurons; NMDA receptors; long-axis

INTRODUCTION

Encoding and consolidating new associative memories requires an intact hippocampal formation (Squire et al., 2004). Spanning the longitudinal extent of the medial temporal lobes, the long-axis is the hippocampus' largest dimension (Small, 2002). The entorhinal cortex, receiving input from all sensory modalities, is the main gateway into the hippocampus (Witter et al., 1989a). Despite significant convergence, studies suggest that sensory input accesses separate divisions of the entorhinal cortex (Witter et al., 1989b), and that the entorhinal cortex differentially relays this input onto separate segments of the hippocampal long-axis (Van Groen and Lopes da Silva, 1985; Witter et al., 1989b; Pare and Llinas, 1994; Dolorfo and Amaral, 1998). This functional organization accounts for findings from a growing number of fMRI (functional magnetic resonance imaging) studies showing that sensory modalities evoke anatomically distinct activation patterns recorded from the hippocampal long-axis (Fig. 1). Specifically, while olfactory (Cerf-Ducastel and Murphy, 2001; Poellinger et al., 2001) and novel auditory stimuli (Crottaz-Herbette et al., 2005; Saykin et al., 1999; Small et al., 2001) are more likely to activate anterior segments of the hippocampal long-axis, novel visual information typically activates more posterior hippocampal segments (Brewer et al., 1998; Crottaz-Herbette et al., 2005; Small et al., 2001; Stern et al., 1996).

In a previous fMRI study using visual and auditory stimuli, we found that sensory-evoked activity recorded from the hippocampal long-axis is not fixed, but rather, is modifiable by experience (Small et al., 2001). Whereas viewing unfamiliar faces evoked a posterior-dominant activation pattern, face-evoked activation shifted to more anterior hippocampal segments after subjects learned to associate faces with names. We interpreted this experience-dependent shift in the context of the unique properties of CA3 hippocampal neurons, properties that form the basis of Marr's computational model of hippocampal function (Marr, 1971) (Fig. 1C). CA3 neurons form extensive connections up and down the hippocampal long-axis (MacVicar and Dudek, 1980; Miles and Wong, 1986) and, importantly, CA3–CA3 connections have been shown to have NMDA-dependent long term potentiation (Harris and Cotman, 1986; Williams and Johnston, 1988; Zalutsky and Nicoll, 1990). Thus, as shown in previous electrophysiological studies (Anderson et al., 1971; Pare and Llinas, 1994), we assumed that once gaining access to select hippocampal segments, face-evoked activity and name-evoked activity spread throughout the hippocampal long-axis. Furthermore, we predicted that when faces and names are paired in time CA3–CA3 LTP binds the activation patterns at the site in the hippocampal long-axis where activation patterns converge (Small, 2002). In fact, in our fMRI study, we found that the anterior shift in long-axis activity emerged during repeated exposure to face–name pairing. Thus,

[1] **Taub Institute for Research on Alzheimer's Disease and the Aging Brain, Department of Neurology, Columbia University College of Physicians and Surgeons, New York, New York; The Picower Institute for Learning and Memory, RIKEN-MIT Neuroscience Research Center, Howard Hughes Medical Institute, Department of Biology, Massachusetts Institute for Technology, Cambridge, Massachusetts;** [2] **The Picower Institute for Learning and Memory, RIKEN-MIT Neuroscience Research Center, Howard Hughes Medical Institute, Department of Brain and Cognitive Sciences, Massachusetts Institute for Technology, Cambridge, Massachusetts**
Grant sponsor: Federal grants; Grant numbers: AG025161, MH058880; Grant sponsor: McKnight Neuroscience.
*Correspondence to: Scott A. Small, 630 West 168th Street, PH 19, NY, 10032. E-mail: sas68@columbia.edu
Accepted for publication 2 May 2007
DOI 10.1002/hipo.20332
Published online in Wiley InterScience (www.interscience.wiley.com).

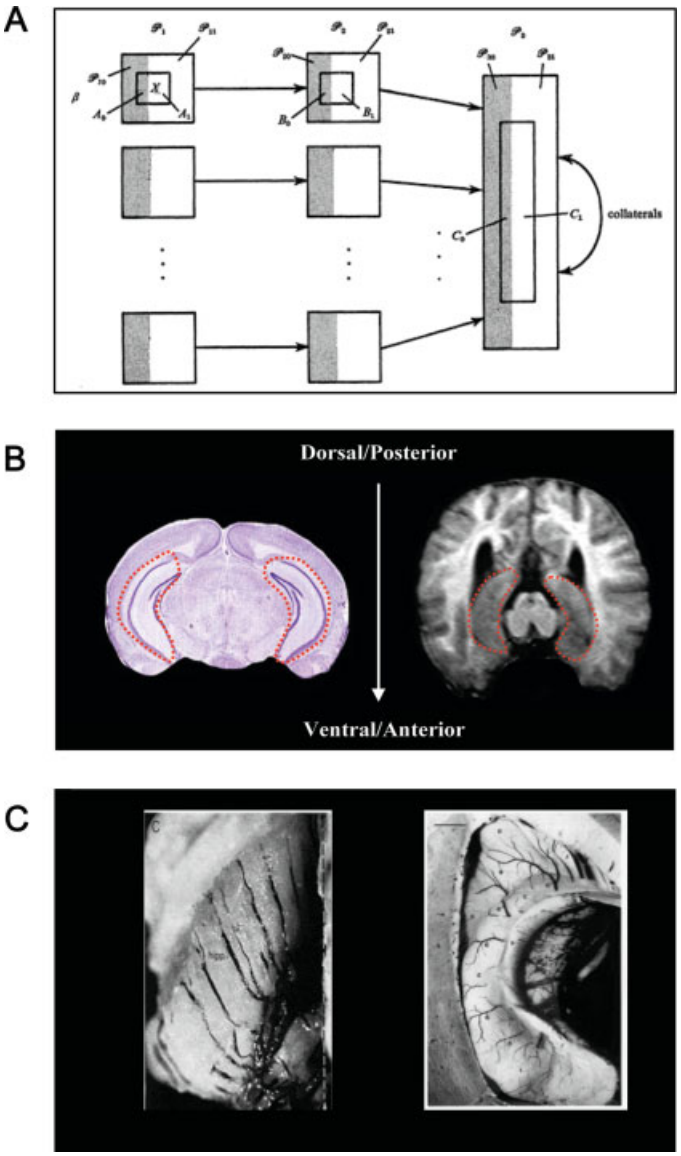

FIGURE 1. The anatomical and functional organization of hippocampal long-axis. A: Marr's computation model of hippocampal function (reprinted with permission from Marr Philos Trans R Soc Lond B Biol Sci, 1971, 262, 23–81, Royal Society of London). The right rectangle represents the hippocampus and the 'collaterals' refer to CA3–CA3 connectivity, organized up and down the hippocampal long-axis. The squares represent separate elements of a complex memory accessing different segments of the hippocampal long-axis. B: Orientations of view. As demonstrated by a histological image (left panel), a coronal orientation is superior for visualizing the hippocampal long-axis in mice (demarcated by the red stippled line). The ventral-to-dorsal orientation of hippocampal long-axis in mice (left panel) is equivalent to the anterior-dorsal orientation of the hippocampal long-axis in humans (demarcated by the stipple line) as shown by MRI (right panel). C. The vascular organization of the hippocampal long-axis informs on its functional organization. Approximately eight circumferential vessels are organized in a parallel fashion spanning the hippocampal long-axis in rodents (left panel) and in humans (right panel).

influenced by Marr's model, we proposed that when subjects were exposed to a face after face–name pairing—i.e., exposed to a "fragment" of the original memory—prior experience-dependent CA3 plasticity may have accounted for the observed shift in peak activation.

If this proposed mechanism is true, then blocking NMDA receptors in CA3 neurons is predicted to prevent the experience-dependent shift in hippocampal long-axis activity. We reasoned, therefore, that recording patterns of long-axis activity in transgenic mice in which CA3 NMDA receptors are selectivity knocked-out (Nakazawa et al., 2002) would be a powerful approach for testing this prediction. To achieve this goal, we first needed to develop an fMRI protocol capable of recording sensory-evoked activity in the hippocampal long-axis of the mouse.

Besides the use of a high-field scanner, addressing a number of imaging-related factors led to the successful development of a mouse-fMRI protocol. First, since peak activation is assumed to be both small and spatially restricted, we explored ways to maximize blood oxygen level dependent (BOLD) signal while preserving spatial resolution. Echo-planar (EPI) pulse sequences are typically used in fMRI studies because of its superior temporal resolution. However, as in all MRI pulse sequences, temporal resolution trades-off with spatial resolution, and EPI pulse sequences typically cannot achieve the sub-millimeter resolution required to visualize selected areas of the mouse hippocampal formation. Furthermore, the high temporal resolution of EPI typically comprises signal-to-noise. In this regard, we were guided by Ogawa's original studies in which non-EPI pulse sequences were used to first show the BOLD effect in the rodent brain (Ogawa et al., 1990a,b). We reasoned that if we could overcome its poorer temporal resolution, non-EPI pulse sequences would provide BOLD maps of the hippocampal long-axis possessing higher signal and superior spatial resolution.

Minimizing head motion is the second imaging issue that needed to be addressed. In principle, three options are available: mechanical constraints, neuromuscular blockade coupled with external ventilation, or "generalized" anesthesia. All three options present potential confounds for imaging brain function. While anesthetic agents, by definition, reduce brain function, the first two options do not minimize the fear and anxiety induced during scanner, which also affect the function of the brain. On balance, we preferred the controlled effect of generalized anesthesia over the uncontrolled effect of fear and anxiety. Indeed, a number of studies have shown that sensory-evoked BOLD can be recorded using anesthetic agents (Lee et al., 1999; Mandeville et al., 2001; Keilholz et al., 2006).

The third factor was developing an activation task that could stimulate the anesthetized hippocampal formation. We decided to rely on odors as the sensory modality of choice. Just two synapses separate the entorhinal cortex from the olfactory bulb, and therefore for anatomical reasons odors, compared to other sensory modalities, are more likely to stimulate the hippocampus. Furthermore, olfactory learning in rodents has additional advantages, such as high acuity and discrimination. Indeed,

previous electrophysiologic studies have shown that even under anesthesia olfactory stimulation can successfully activate the hippocampal formation (Heale and Vanderwolf, 1994). Finally, as a last imaging-related factor, we anticipated that physiologic parameters such as pulmonary and cardiovascular function might be affected by anesthetic agents. Since this variance can potentially affect the BOLD signal (Steward et al., 2005), these sources of noise needed to be addressed. Toward this end, we carefully monitored physiological parameters during scanning and applied strict criteria for physiologic stability.

Here, we introduce our mouse-fMRI protocol, and show that, as in humans, odors evoke ventral-predominant activation of the hippocampal long-axis. More importantly, we find that odor-evoked activity can shift in an experience-dependent manner. Finally, we show that experience-dependent shift in hippocampal long-axis activity is blocked in transgenic mice which do not express NMDA-receptors in CA3 neurons.

METHODS

Image Acquisition

All scanning was performed with an 89-mm bore 9.4 T vertical Bruker magnet (AVANCE 400WB spectrometer; Bruker NMR, Billerica, MA) using a 30-mm-i.d birdcage RF probe and a shielded gradient system (100 G/cm).

Although inhalant anesthetics, such as isoflurane, have been used in prior rodent fMRI studies (Steward et al., 2005), these agents are typically odorous. Instead, we anesthetized mice with intraperitoneal (i.p.) injections of ketamine/xylazine, which in contrast to most other anesthetics, has the added advantage of not affecting hemodynamic coupling (Crosby et al., 1982; Cavazzuti et al., 1987). All mice were initially anesthetized with IP injections of ketamine (75 mg/kg) and xylazine (3.75 mg/kg). A PE10 polyethylene tubing (O.D. 024") was introduced into the peritoneal cavity and sutured, allowing for injecting maintenance dosage of ketamine/xylazine over the course of the imaging session. Repeated injections during scanning were administered to minimize the stimulatory effect of low ketamine doses (Hammer and Herkenham, 1983).

Three scout scans were first acquired to reproducibly position the mouse brain in a standard anatomical orientation. Gradient-echo acquisition parameters were TR/TE = 40/5.5, flip angle = 5°, matrix = 192 × 256, slice thickness = 0.6 mm, slice gap = 0.2 mm, and NEX = 1, with each acquisition lasting 66 s. Spin–echo acquisition parameters were TR/TE = 4,000/9, NEX = 1, matrix = 256 × 256, slice thickness = 0.6 mm.

The details of the activation protocol were empirically derived. First, in exploratory studies, we tested different acquisition times and found that an acquisition time of 66 s was the shortest period with which we could acquire high-quality gradient-echo images of the mouse brain. Accordingly, the "activation cycle" used in our activation protocol consisted of an odor phase ("on"), lasting 66 s, alternating with a room-air phase ("off") lasting 5.5 min. For our initial studies, we used vaporized iso-amyl acetate ("banana"), a non-noxious odor that is relatively novel to laboratory mice. Although the BOLD signal is improved by increasing the number of the activation cycles, the BOLD response to odors has a complicated habituation pattern (Poellinger et al., 2001; Sobel et al., 2000). Thus, we empirically determined the optimum number of activation cycles, guided by the level of BOLD activation observed in primary and secondary olfactory cortex as visualized in sagital slices. We found that a single activation cycle (off-on-off) generated the most robust activation in olfactory cortex.

Mice were carefully monitored during scanning and individual experiments were rejected for physiological instability during scanning: heart rate was monitored via ECG (SM 785, Bruker), with subcutaneous silver electrodes attached to front limbs and a reference electrode attached to the right posterior limb; respiratory rate was measured via a pressure transducer outfitted within the RF coil (Bruker); SaO_2 was monitored using pulse oximetry (Model V33304, Sergivet), with the probe attached to a shaven region in the lower abdomen; and, rectal temperature was monitored with a thermestor (YSI Precision Thermometer 4000A). In preliminary studies, we have found that a 20% reduction in the respiratory rate was the most reliable indicator of cardiopulmonary instability, and thus, when observed, this reduction was applied as an exclusionary criterion. Experiments in 34% of mice were rejected because of cardiopulmonary instability.

Odor Delivery

Liquid forms of the odors were first vaporized in a 60-ml syringe. Then, the vaporized odor was injected into the outflow plastic tubing (5 mm in diameter) attached to a mechanical respiration pump (model 607; Harvard Apparatus, Cambridge, MA), flowing air at a rate of 2 l/min. The injection was made as close as possible to animal's location within the magnet, ~1 m away. The tubing was connected to a plastic cone, 15 mm in diameter, that snuggly fits over the animal's snout, thereby delivering the odor.

Behavioral Training and Testing

In contrast to humans, multiple sensory modalities cannot be used during mouse scanning and so training and testing were performed outside the magnet. A modified context fear conditioning paradigm was used for training. "Context" has been defined as an environment comprised separate sensory modalities (Rudy and O'Reilly, 1999, 2001)—consisting typically of visuospatial and olfactory elements—and the ability to learn a context requires hippocampal-dependent binding of these individual elements.

Mice were conditioned in a mouse fear conditioning chamber (MED-AFC-M1, Med-Associates, St. Albans, VT) equipped with a shock grid floor. Actimetrics FreezeFrame (Evanston, IL) software was used to quantify freezing, as recorded via a CCD video camera connected to a PC workstation. Two separate "contexts" were designed. The visuospatial

cues of Context A and Context B differed by changing the color (from silver to white) and the shape of the back wall of the chamber (from straight to curved), and by changing the chamber's lighting (from white to red). A high concentration infusion of a well-defined odor was a modification over conventional paradigms. Specifically, iso-amyl acetate infusions was the defining odor of Context A, while (−)-carvone infusions was the defining odor of Context B.

The timeline of the experimental paradigm was as follows: One group of mice ($n = 8$) was trained in Context A and the other group ($n = 8$) was trained in Context B. Training consisted of a 15-min session during which three 2-s foot shocks were delivered via shock grid (0.7 mA). Shock administration began 7.5 min after the animals were placed in each context. Forty-eight hours later, both groups of mice were imaged with the fMRI odor-activation protocol, using iso-amyl acetate as the olfactory stimulant. Then, 6 h after repeat scanning all mice were placed in Context A for 4 min, and the average posttraining freezing time was recorded.

The 52-h delay between training and testing is another modification over conventional context fear conditioning paradigms. Context fear conditioning has both a hippocampal and amygdala component (Petrovich et al., 2001), and we were particularly concerned about amygdala input since it accesses ventral segments of the hippocampal long-axis (Petrovich et al., 2001). Although not definitive, previous studies have suggested that imposing a long delay increases the odds that posttraining freezing is dependent on the hippocampus (Phillips and LeDoux, 1992).

Pretraining freezing was quantified by averaging the per-minute freezing times for the 4 min prior to the first foot shock. Posttraining freezing (52 h later) was quantified by averaging the per-minute freezing times for the 4 min the mice spent in Context A.

Data Analysis

All image analysis was performed using the MEDx (Sensor Systems) software program. Each study was motion corrected and signal intensity was normalized but not spatially filtered. For each individual study, a *z*-score map was generated comparing the images acquired during the "on" odor phases compared with images acquired from the "off" room-air phases.

For purposes of visual inspection, two graphical representations of mean activation were generated, illustrating the averaged pattern of hippocampal activation for all subjects within a given experimental condition. First, mean activation maps were generated by co-registering and averaging *z*-score maps from individual studies. To highlight areas of greatest activation, an arbitrary threshold of *z*-score ≥ 2 was applied to the mean activation map, and the derived maps were color coded in red. Second, to illustrate the full range of activation, numerical line-graphs were generated using a line function applied to unthresholded mean *z*-score maps from a particular experiment. The line function covered the medial-lateral extent of the hippocampus, and the graphs were generated to show the full pattern of long-axis activation.

For between-group statistics, data reduction was performed on the activation data acquired over the full extent of the hippocampal long-axis. In doing so, we were guided by the eight separate circumferential vessels, organized in a parallel fashion spanning the ventral-to-dorsal hippocampal long axis (Fig. 1B), that have been invoked to account for the functional organization of the hippocampal long-axis (Anderson et al., 1971). Accordingly, the following segmentation procedure was performed, on a mouse-by-mouse basis, by an investigator blinded to experimental grouping. First, from the series of coronal anatomical MR images, the image that provides superior visualization of the hippocampal long-axis is identified; this image was equivalent across animals (For examples, see Figs. 2B, 3A, or 4A). The anatomical contrast generated in these images is sufficient to visualize and outline the boundaries of the hippocampal long-axis. Then, relying on this anatomical information, the outline tool in MEDx is used to carefully demarcate the full extent of the hippocampal long-axis (For examples, see Figs. 2B, 3A, or 4A). Next, the line-function tool in MEDx is used to measure activation *z*-scores along the full hippocampal long-axis. Because of the curvature of the hippocampal long-axis, three consecutive lines-functions are used. The first is placed within the lower curvature of the hippocampal long-axis (a "north-east" pointing line); the second is placed within the vertical section of the hippocampal long-axis (a "north" pointing line); and the third is placed within the upper curvature of the hippocampal long-axis (a "north-west" pointing line). The measurements from these three lines are concatenated and transferred to a single column in an Excel worksheet. In all cases, the full extent of hippocampal long-axis was made up of 48–53 data points (examples are shown in Fig. 3A); therefore, the column was binned into eight sequential segments, and the mean *z*-score from each of the eight bins was used in group data analysis. The group data was analyzed with a repeated-measure ANOVA, using a between-group polynomial contrast. The average activation measured from each of the eight long-axis segments was included as the within-subject factors, and group (prior-experience vs. no-experience) was included as the between-group factor.

RESULTS

Imaging Sensory-Evoked Activity in the Mouse Hippocampus

The activation protocol (as described in the Methods section) was empirically driven, optimizing parameters based on degree of activation observed in sagital slices of the brain. Using this protocol, BOLD activation was observed in the primary olfactory cortex—the olfactory bulbs—as well as in secondary olfactory cortex consisting of the piriform cortex and ventral medial temporal lobes (either entorhinal cortex or ventral hippocampus) (Fig. 2A). Furthermore, in agreement with

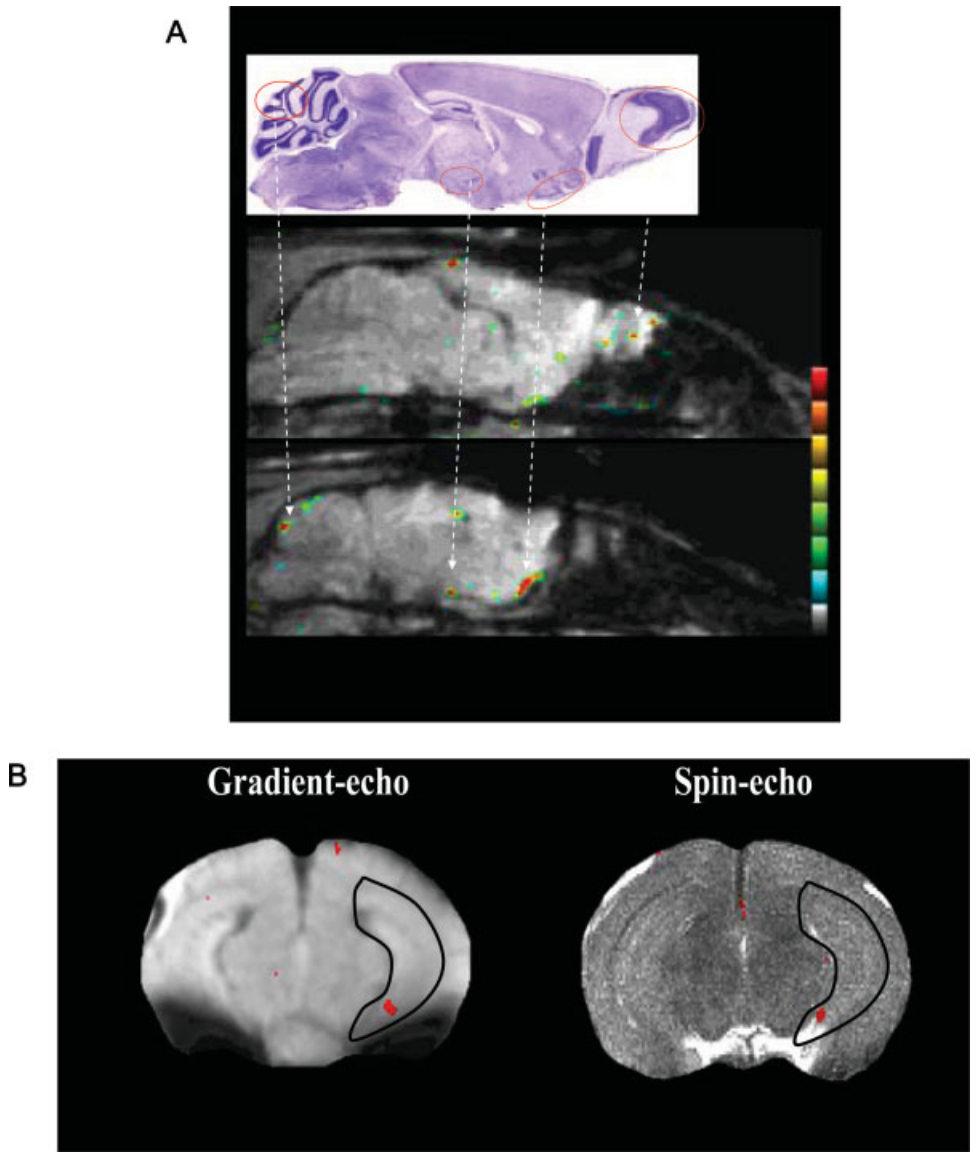

FIGURE 2. Odor-evoked activity observed in the ventral hippocampus. A: A sagital histological slice (upper panel) identifies (from right to left) the olfactory bulb, the piriform cortex, the ventral medial temporal lobe, and the cerebellum. A medial sagital image (middle panel) shows activity in the olfactory bulb. A lateral sagital image (lower panel) shows activity in the piriform cortex, ventral medial temporal lobes, and the cerebellum. Images were generated by overlaying a thresholded statistical map reflecting BOLD changes induced by an odor ($N = 8$) onto a mean anatomical image. B: Gradient-echo axial images (left panel) demonstrate that peak odor-evoked activity occurs in the ventral left hippocampal long-axis. Spin–echo axial images (right panel) confirm that peak odor-evoked activation occurs in the ventral left hippocampal long-axis.

fMRI studies in humans and monkeys (Boyett-Anderson et al., 2003; Sobel et al., 1998), we found that odors stimulated the mouse cerebellum.

Human fMRI studies have documented that odors differentially activate the anterior hippocampus, which is equivalent to the ventral hippocampus of mice (Fig. 1A). In mice, axial slices better visualize the full longitudinal extent of the hippocampus (Fig. 1A) (Dolorfo and Amaral, 1998; Paxinos and Franklin, 2001), and we therefore replicated the odor activation experiment but acquired axial instead of sagital images. In this orientation, we reliably identified a single slice that best visualized the full hippocampal long-axis (Fig. 2B). Indeed, the greatest odor-evoked activation was observed in the ventral hippocampus (Fig. 2B, left panel).

As shown, ventral activity was most prominent in the left hippocampus. Since susceptibility artifact might have contributed to this lateralization effect, which as in humans, can obscure the ventral temporal lobes (Fig. 2B, left panel), we decided to repeat the experiment using spin–echo instead of gradient-echo pulse sequences. Besides reducing susceptibility artifact, spin–echo BOLD has an additional advantage of reflecting small, rather than large, vessel deoxyhemoglobin content (Boxerman et al.,

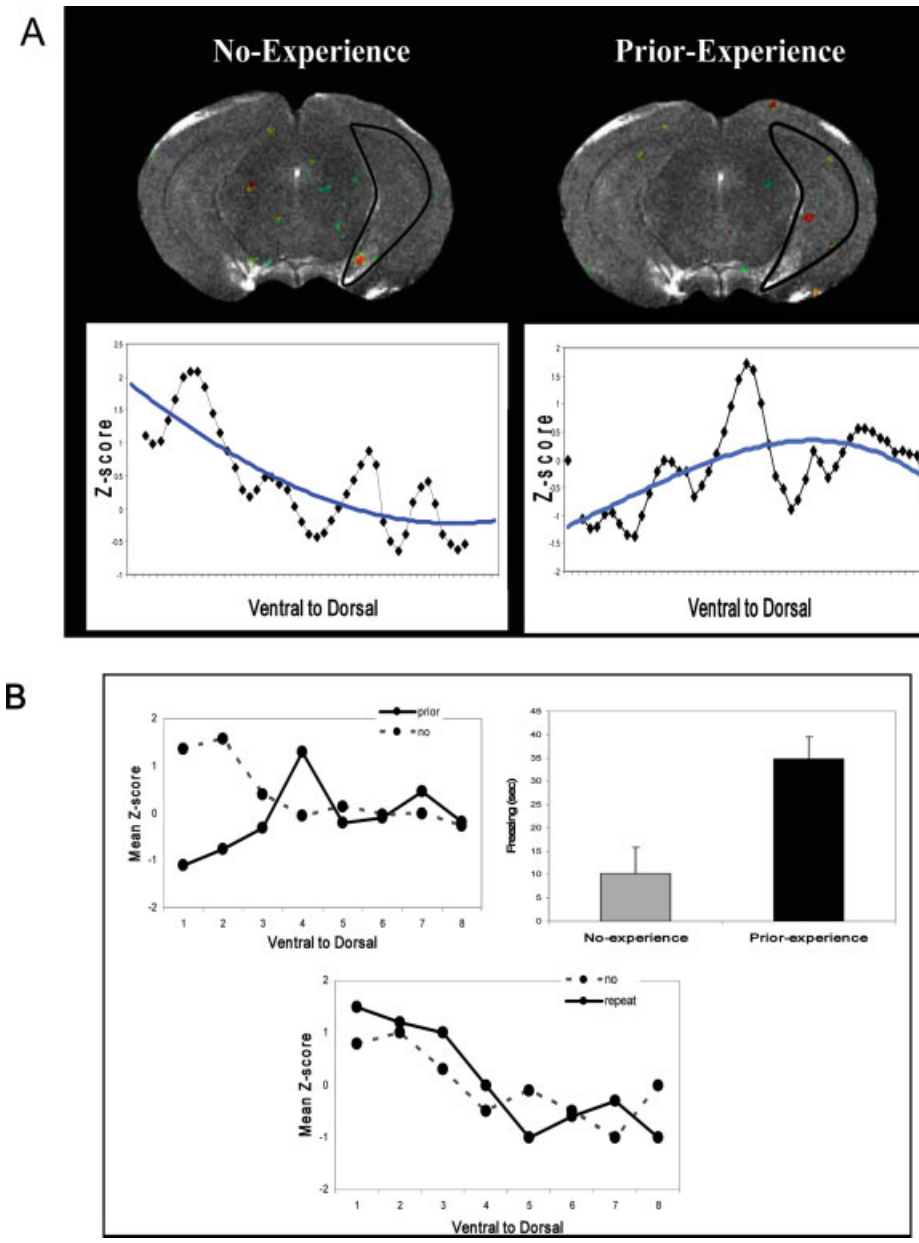

FIGURE 3. Odor-evoked hippocampal activity shifts dorsally in an experience-dependent manner. A: Compared to no-experience (left panel), prior-experience caused a dorsal shift in odor-evoked hippocampal activity (right panel). Corresponding graphs show the activation pattern recorded from the full extent of the hippocampal long-axis. B: Mean activation from the eight hippocampal segments (left panel), organized from ventral-to-dorsal, for the prior-experience group (solid line) and for the no-experience group (stippled line). Posttraining freezing times (right panel), averaged across 4 min, for the no-experience group (gray bar) and the prior-experience group (black bar). Mean activation from the eight hippocampal segments (lower panel), organized from ventral-to-dorsal, are shown for the first-exposure group (solid line) and for first-exposure group (stippled line).

1995; Lee et al., 1999; Oja et al., 1999; Keilholz et al., 2006). As in the first series of experiments, odor-evoked activation was highest in the ventral hippocampus, which again was most reliably observed on the left (Fig. 2B, right panel). Although we cannot exclude technical reasons for this lateralizing effect, we nevertheless focused on the reliable odor-evoked activity in the left ventral hippocampus for the next series of experiments.

Experience-Dependent Shift in Odor-Evoked Activity

Once we established a sensory-evoked activation pattern in the mouse hippocampal long-axis, we were interested to determine whether, as in humans, this activation pattern can be shifted by prior experience. A modified context fear conditioning paradigm was used whose goal was to bind olfactory stimuli with

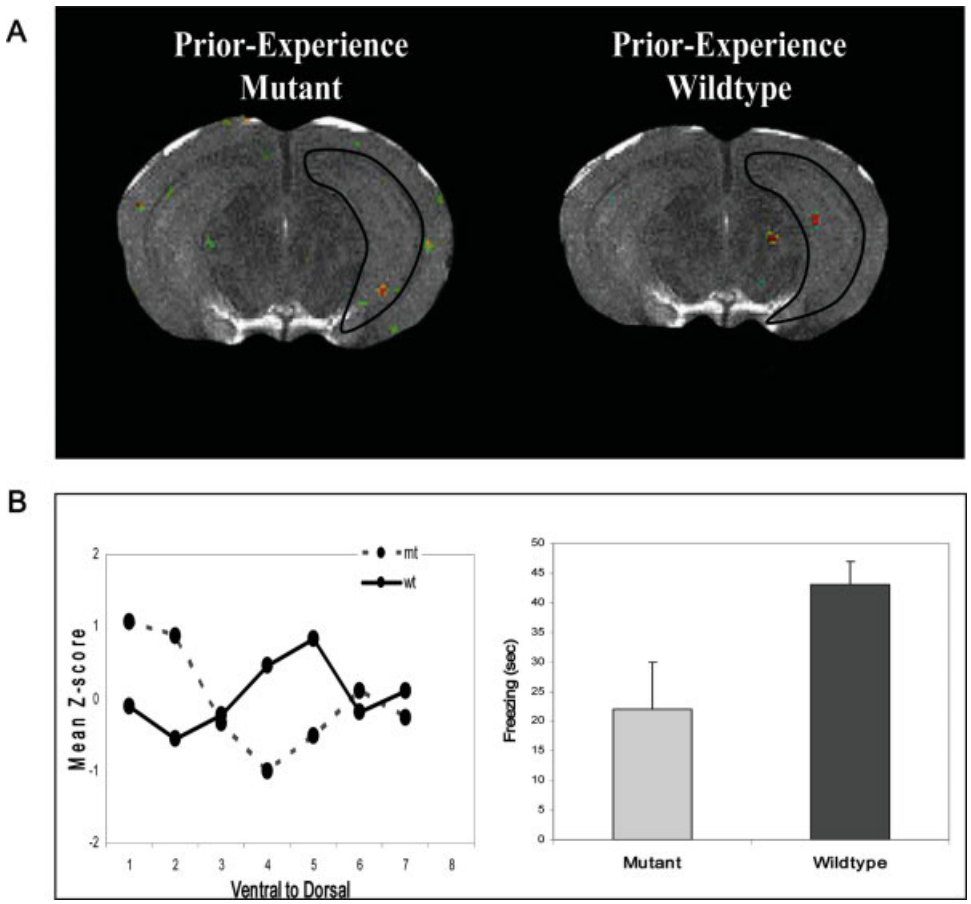

FIGURE 4. The experience-dependent shift in odor-evoked activity is blocked in CA3-NR1 knock-out mice A. In contrast to wildtype littermates (right panel), the experience-dependent shift in odor-evoked activity was blocked in mutant mice (left panel). B: Mean activation from the eight hippocampal segments (left panel), organized from ventral-to-dorsal, for the wildtype group (solid line) and for the mutant group (stippled lines). Posttraining freezing times (right panel), averaged across 4 min, for the mutants (gray bar) and the wildtype littermates (black bar).

visuospatial stimuli, which preferentially access the dorsal hippocampus (Jung et al., 1994). The two main modifications over conventional paradigms were the use of high-concentrations of a well defined odor, and imposing a 52-h delay between training and testing in an attempt to reduce the amygdala component of contextual learning (Phillips and LeDoux, 1992).

Peak activation in response to odor was observed to shift dorsally in mice which received prior experience with iso-amyl acetate, but not in mice that received prior experience with (−)-carvone (Fig. 3A). Results of this analysis showed a significant group X long-axis interaction ($F = 11.1$; $P \leq 0.05$) (Fig. 3B), confirming that prior-experience shifted the activation dorsally. Pretraining freezing was not different between the groups, but posttraining freezing was significantly increased in the mice who trained in Context A (prior experience) compared with mice who trained in Context B (no-experience) ($t = 3.6$; $P \leq 0.01$) (Fig. 3B).

To partially address whether familiarity alone could account for the effect, we imaged a new group of mice ($n = 8$), using iso-amyl acetate, and then repeated the experiment 48 h later. Prior exposure to iso-amyl acetate in the anesthetized state did not cause a dorsal shift in hippocampal activity ($F = 0.81$) (Fig. 3B; bottom panel).

Experience-Dependent Shift in Odor-Evoked Activity is Blocked in CA3-NRI Knock-Out Mice

Once established in wild-type mice, we next tested for an experience-dependent shift in hippocampal long-axis activity in CA3-NR1 knock-out mice and their wild-type littermates. As previously described, the CA3 NMDA receptor is knocked-out in the mutant mice throughout the hippocampal long-axis (Nakazawa et al., 2002). As in the "prior-experience" group described above, both mutant ($n = 6$) and wild-type ($n = 8$) mice were trained in Context A, were scanned 48 h later using iso-amyl acetate as the stimulant, and then, 6 h after scanning, were behaviorally tested in Context A.

An experience-dependent shift in hippocampal activity was observed in wild-type mice, but not in mutant mice (Fig. 4A). A repeated-measures MANOVA, comparing the activation patterns of mutant vs. wild-type mice, revealed a significant group X

long-axis interaction ($F = 9.4$; $P \leq 0.05$) (Fig. 4B, left panel). The wild-type and mutant mice did differ in pretraining freezing, but the compared to mutant mice, wild-type mice showed greater posttraining freezing ($t = 2.4$; $P \leq 0.05$) (Fig. 4B, right panel). These results confirm that the 52 delay used in the behavioral protocol was at least partially hippocampal-dependent.

DISCUSSION

In this study, a mouse-fMRI protocol was optimized so that a circuit-based hypothesis about of the function of the hippocampal long axis could be tested. The origins of this hypothesis are attributed to Marr's computational model of hippocampal function (Fig. 1A). In that model, the unique "associative" connections that interconnect CA3 neurons were used to suggest how the hippocampus might function (Marr, 1971). Specifically, once individual elements of a complex memory accesses different segments of the hippocampus, the model predicts that CA3–CA3 connections bind these elements in an experience-dependent manner. Then, during memory retrieval, exposure to one element is predicted to reactivate the full memory as encoding in the hippocampus. Although not specifically articulated in Marr's model, when interpreted in the context of the established anatomical organization of the hippocampus, the model would predict that exposure to a memory fragment after memory encoding should result in an anatomical shift in long-axis activity. At a molecular level, this shift is predicted to be governed by CA3–CA3 LTP, and therefore to be mediated by CA3 NMDA receptors. Of note, many additional and more elaborate computational models of hippocampal function have been proposed since Marrs' time (O'Reilly and McClelland, 1994; Treves and Rolls, 1994; Wallenstein et al., 1998), but most still incorporate the unique autoassociative nature of CA3 neurons in developing their models. Interestingly, in contrast to the Marr's model, many of the more recent models de-emphasize the actual anatomy of the hippocampus, in particular the fact that the CA3–CA3 associative tracts extends up and down the hippocampal long-axis (Small, 2002).

Although possible, testing for long-axis shifts in evoked activity is challenging relying on standard electrophysiology. As we have shown, when designed with this specific question in mind, fMRI is well-suited for mapping the pattern of sensory-evoked activation recorded over the full extent of the hippocampal long-axis. Establishing in mice that CA3 NMDA receptors are required for the experience-dependent shift in sensory-evoked activity provides empirical validation, both for Marr's general model and for our specific hypothesis. This validation, in turn, provides a conceptual framework with which to interpret suggesting the manner in which the experience-dependent shift in sensory-evoked activity contributes to the mnemonic function of the hippocampus.

As illustrated in this study, combining the technologies of fMRI and transgenic engineering is powerful in addressing molecular and cellular questions about the underlying mechanisms that mediate functional brain maps. Nevertheless, there are a number of limitations to mouse fMRI. Key among these are the limited repertoire of behavioral tasks that can be used during scanning, a limitation compounded by the requirement for anesthesia. So, for example, we currently cannot use visuospatial stimulants during imaging, and thus we relied on prior studies whose results suggest that visuospatial information preferentially accesses the dorsal segments of the hippocampal long-axis. Furthermore, we postulate that the observed experience-dependent shift is not simply caused by increased familiarity associated with prior exposure to the odor alone. Although we found that under anesthesia, repeated exposure to the odor did not cause a long-axis shift, this nevertheless does not exclude conscious familiarity as a contributor to the observed effect. Additionally, the BOLD signal is extremely sensitive to physiological fluctuations in cardiopulmonary function, and indeed we found that many experiments were rejected because of uncontrolled fluctuations.

Despite these limitations, by applying BOLD fMRI to transgenically engineered mice the findings inform our mechanistic understanding of observed shifts in long-axis activity. First, because the molecular "lesion" in the CA3-NR1 mutant mice is anatomically restricted, the current study suggests that the experience-dependent shift is in fact a hippocampal-dependent event. Furthermore, because context conditioning has an amygdala component, the results observed in the CA3-NR1 mutant mice confirm that the experience-dependent shift is a process that occurs within the hippocampus itself. More importantly, it is only by imaging transgenic mice with selective cellular and molecular defects that we were able to test and confirm the proposed cellular/molecular hypothesis: that CA3 NMDA receptors are required for the experience-dependent shift in hippocampal long-axis activity.

Acknowledgment

Mark Albers is thanked for his aid in developing the olfactory stimulation task.

REFERENCES

Anderson P, Bliss TV, Skrede KK. 1971. Lamellar organization of hippocampal pathways. Exp Brain Res 13:222–238.

Boxerman JL, Hamberg LM, Rosen BR, Weisskoff RM. 1995. MR contrast due to intravascular magnetic susceptibility perturbations. Magn Reson Med 34:555–566.

Boyett-Anderson JM, Lyons DM, Reiss AL, Schatzberg AF, Menon V. 2003. Functional brain imaging of olfactory processing in monkeys. Neuroimage 20:257–264.

Brewer JB, Zhao Z, Desmond JE, Glover GH, Gabrieli JD. 1998. Making memories: Brain activity that predicts how well visual experience will be remembered [see comments]. Science 281:1185–1187.

Cavazzuti M, Porro CA, Biral GP, Benassi C, Barbieri GC. 1987. Ketamine effects on local cerebral blood flow and metabolism in the rat. J Cereb Blood Flow Metab 7:806–811.

Cerf-Ducastel B, Murphy C. 2001. fMRI activation in response to odorants orally delivered in aqueous solutions. Chem Senses 26:625–637.

Crosby G, Crane AM, Sokoloff L. 1982. Local changes in cerebral glucose utilization during ketamine anesthesia. Anesthesiology 56:437–443.

Crottaz-Herbette S, Lau KM, Glover GH, Menon V. 2005. Hippocampal involvement in detection of deviant auditory and visual stimuli. Hippocampus 15:132–139.

Dolorfo CL, Amaral DG. 1998. Entorhinal cortex of the rat: Organization of intrinsic connections. J Comp Neurol 398:49–82.

Hammer RP Jr, Herkenham M. 1983. Altered metabolic activity in the cerebral cortex of rats exposed to ketamine. J Comp Neurol 220:396–404.

Harris EW, Cotman CW. 1986. Long-term potentiation of guinea pig mossy fiber responses is not blocked by *N*-methyl D-aspartate antagonists. Neurosci Lett 70:132–137.

Heale VR, Vanderwolf CH. 1994. Dentate gyrus and olfactory bulb responses to olfactory and noxious stimulation in urethane anaesthetized rats. Brain Res 652:235–242.

Jung MW, Wiener SI, McNaughton BL. 1994. Comparison of spatial firing characteristics of units in dorsal and ventral hippocampus of the rat. J Neurosci 14:7347–7356.

Keilholz SD, Silva AC, Raman M, Merkle H, Koretsky AP. 2006. BOLD and CBV-weighted functional magnetic resonance imaging of the rat somatosensory system. Magn Reson Med 55:316–324.

Lee SP, Silva AC, Ugurbil K, Kim SG. 1999. Diffusion-weighted spin-echo fMRI at 9.4 T: Microvascular/tissue contribution to BOLD signal changes. Magn Reson Med 42:919–928.

MacVicar BA, Dudek FE. 1980. Local synaptic circuits in rat hippocampus: Interactions between pyramidal cells. Brain Res 184:220–223.

Mandeville JB, Jenkins BG, Kosofsky BE, Moskowitz MA, Rosen BR, Marota JJ. 2001. Regional sensitivity and coupling of BOLD and CBV changes during stimulation of rat brain. Magn Reson Med 45:443–447.

Marr D. 1971. Simple Memory: A theory for archicortex. Philos Trans R Soc Lond B Biol Sci 262:23–81.

Miles R, Wong RK. 1986. Excitatory synaptic interactions between CA3 neurones in the guinea-pig hippocampus. J Physiol 373:397–418.

Nakazawa K, Quirk MC, Chitwood RA, Watanabe M, Yeckel MF, Sun LD, Kato A, Carr CA, Johnston D, Wilson MA, Toneqawa S. 2002. Requirement for hippocampal CA3 NMDA receptors in associative memory recall. Science 297:211–218.

Ogawa S, Lee TM, Kay AR, Tank DW. 1990a. Brain magnetic resonance imaging with contrast dependent on blood oxygenation. Proc Natl Acad Sci USA 87:9868–9872.

Ogawa S, Lee TM, Nayak AS, Glynn P. 1990b. Oxygenation-sensitive contrast in magnetic resonance image of rodent brain at high magnetic fields. Magn Reson Med 14:68–78.

Oja JM, Gillen J, Kauppinen RA, Kraut M, van Zijl PC. 1999. Venous blood effects in spin-echo fMRI of human brain. Magn Reson Med 42:617–626.

O'Reilly RC, McClelland JL. 1994. Hippocampal conjunctive encoding, storage, and recall: Avoiding a trade-off. Hippocampus 4:661–682.

Pare D, Llinas R. 1994. Non-lamellar propagation of entorhinal influences in the hippocampal formation: Multiple electrode recordings in the isolated guinea pig brain in vitro. Hippocampus 4:403–409.

Paxinos G, Franklin K. 2001. The Mouse Brain in Stereotaxic Coordinates. San Diego, CA: Academic Press.

Petrovich GD, Canteras NS, Swanson LW. 2001. Combinatorial amygdalar inputs to hippocampal domains and hypothalamic behavior systems. Brain Res Brain Res Rev 38:247–289.

Phillips RG, LeDoux JE. 1992. Differential contribution of amygdala and hippocampus to cued and contextual fear conditioning. Behav Neurosci 106:274–285.

Poellinger A, Thomas R, Lio P, Lee A, Makris N, Rosen BR, Kwong KK. 2001. Activation and habituation in olfaction—an fMRI study. Neuroimage 13:547–560.

Rudy JW, O'Reilly RC. 1999. Contextual fear conditioning, conjunctive representations, pattern completion, and the hippocampus. Behav Neurosci 113:867–880.

Rudy JW, O'Reilly RC. 2001. Conjunctive representations, the hippocampus, and contextual fear conditioning. Cogn Affect Behav Neurosci 1:66–82.

Saykin AJ, Johnson SC, Flashman LA, McAllister TW, Sparling M, Darcey TM, Moritz CH, Guerin SJ, Weaver J, Mamourian A. 1999. Functional differentiation of medial temporal and frontal regions involved in processing novel and familiar words: An fMRI study. Brain 122 (Part 10):1963–1971.

Small S, Nava A, DeLaPaz R, Mayeux R, Stern Y. 2001. Circuit mechanisms underlying memory encoding and retrieval in the long axis of the hippocampal formation. Nat Neurosci 4:442–449.

Small SA. 2002. The longitudinal axis of the hippocampal formation: Its anatomy, circuitry, and role in cognitive function. Rev Neurosci 13:183–194.

Sobel N, Prabhakaran V, Hartley CA, Desmond JE, Zhao Z, Glover GH, Gabrieli JD, Sullivan EV. 1998. Odorant-induced and sniff-induced activation in the cerebellum of the human. J Neurosci 18:8990–9001.

Sobel N, Prabhakaran V, Zhao Z, Desmond JE, Glover GH, Sullivan EV, Gabrieli JD. 2000. Time course of odorant-induced activation in the human primary olfactory cortex. J Neurophysiol 83:537–551.

Squire LR, Stark CE, Clark RE. 2004. The medial temporal lobe. Annu Rev Neurosci 27:279–306.

Stern CE, Corkin S, Gonzalez RG, Guimaraes AR, Baker JR, Jennings PJ, Carr CA, Sugiura RM, Vedantham V, Rosen BR. 1996. The hippocampal formation participates in novel picture encoding: Evidence from functional magnetic resonance imaging. Proc Natl Acad Sci USA 93:8660–8665.

Steward CA, Marsden CA, Prior MJ, Morris PG, Shah YB. 2005. Methodological considerations in rat brain BOLD contrast pharmacological MRI. Psychopharmacology (Berl) 180:687–704.

Treves A, Rolls ET. 1994. Computational analysis of the role of the hippocampus in memory. Hippocampus 4:374–391.

Van Groen T, Lopes da Silva FH. 1985. Septotemporal distribution of entorhinal projections to the hippocampus in the cat: Electrophysiological evidence. J Comp Neurol 238:1–9.

Wallenstein GV, Eichenbaum H, Hasselmo ME. 1998. The hippocampus as an associator of discontiguous events. Trends Neurosci 21:317–323.

Williams S, Johnston D. 1988. Muscarinic depression of long-term potentiation in CA3 hippocampal neurons. Science 242:84–87.

Witter MP, Groenewegen HJ, Lopes da Silva FH, Lohman AH. 1989a. Functional organization of the extrinsic and intrinsic circuitry of the parahippocampal region. Prog Neurobiol 33:161–253.

Witter MP, Van Hoesen GW, Amaral DG. 1989b. Topographical organization of the entorhinal projection to the dentate gyrus of the monkey. J Neurosci 9:216–228.

Zalutsky RA, Nicoll RA. 1990. Comparison of two forms of long-term potentiation in single hippocampal neurons. Science 248: 1619–1624.